

**Electronic Supplementary Information for: Detection of *Pseudomonas aeruginosa* quorum sensing molecules at an electrified liquid|liquid micro-interface through facilitated proton transfer.**

Edward D. Burgoyne,<sup>a</sup> Andrés F. Molina-Osorio,<sup>a</sup> Reza Moshrefi,<sup>b</sup> Rachel Shanahan,<sup>c</sup> Gerard P. McGlacken,<sup>c</sup> Talia Jane Stockmann,<sup>b,\*</sup> and Micheál D. Scanlon<sup>a,\*</sup>

<sup>a</sup> The Bernal Institute and Department of Chemical Sciences, School of Natural Sciences, University of Limerick (UL), Limerick V94 T9PX, Ireland

<sup>b</sup> Memorial University of Newfoundland, Chemistry Department, 283 Prince Philip Dr., St. John's, NL Canada A1B 3X7

<sup>c</sup> School of Chemistry and Analytical and Biological Chemistry Research Facility (ABCRF), University College Cork, College Road, Cork, Ireland

\*Email: [tstockmann@mun.ca](mailto:tstockmann@mun.ca) (T.J.S)

\*Email: [micheal.scanlon@ul.ie](mailto:micheal.scanlon@ul.ie) (M.D.S)

**Table of Contents**

1. Electrochemical determination of microchannel radius.
2. Asymmetric Diffusion Regime
3. Investigation of proton sources on ligand complexation
4. Cyclic voltammetric response moving from  $[H^+] \gg [ligand]$  to the  $[H^+] \approx [ligand]$  regime
5. Linear Regression Error analysis.

## 1. Determination of microchannel radius

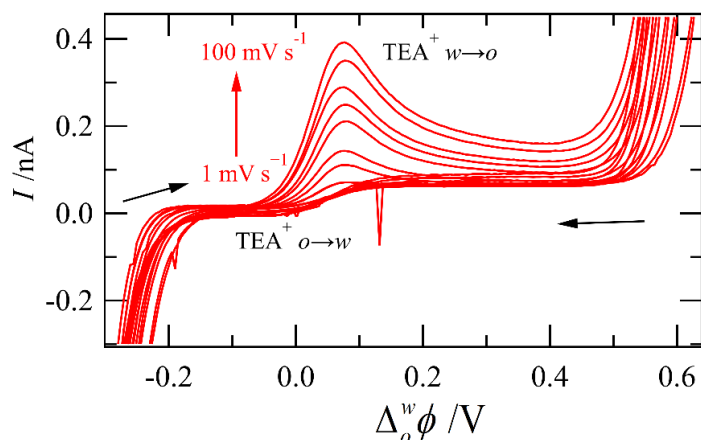


**Figure S1:** Cyclic voltammograms obtained using Cell S1 and varying the scan rate from 1-100  $\text{mV s}^{-1}$ .

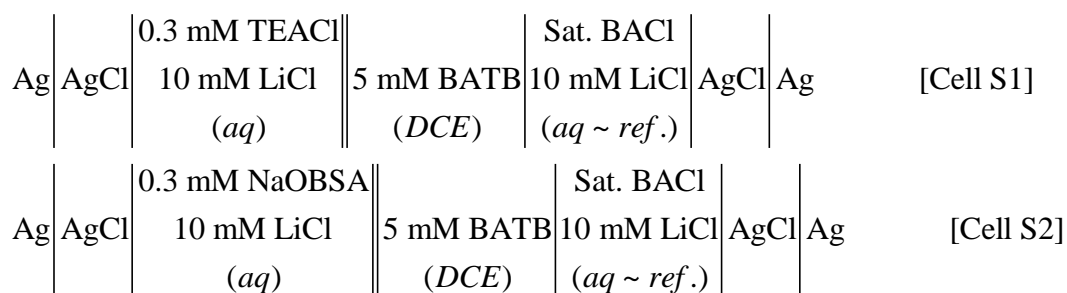
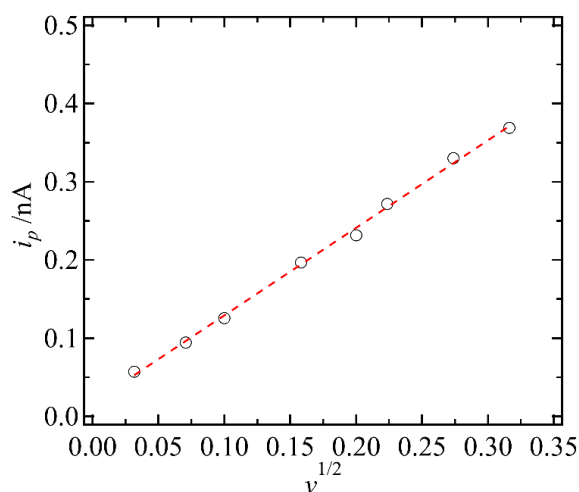


Figure S1 shows the CVs generated using Cell S1 and by scanning the potential between roughly  $-0.35$  and  $0.55$  V. During the forward scan (from low to high potentials) a peak-shaped wave was observed with a half-wave potential at  $0.049$  V.<sup>1</sup> Meanwhile, a steady state or s-shaped wave was observed when scanning from  $0.55$  V to  $-0.35$  V. Owing to the asymmetric geometry of the capillary, this leads to linear diffusion of ions leaving the pipette (crossing the interface from  $w \rightarrow o$ , egress) and hemispherical diffusion of ions entering the pipette (crossing the interface from  $o \rightarrow w$ , ingress). Therefore, the peak-shaped wave is the transfer of  $\text{TEA}^+$  from  $w \rightarrow o$ , while the sigmoidal wave is the ingress of  $\text{TEA}^+$  from  $o \rightarrow w$ .

The radius of the microchannel formed at the tip of the pulled borosilicate glass capillary was confirmed using cyclic voltammetric (CV) measurements of the peak-shaped ion transfer wave of tetraethylammonium ( $\text{TEA}^+$ ) from  $w \rightarrow o$  by varying the scan rate ( $\nu$ ) as shown in Figure S1 and comparing the change in peak current intensity ( $i_p$ ) in amperes to the Randles-Sevcik equation<sup>2</sup> below,

$$i_p = 0.4463 \left( \frac{F^3}{RT} \right)^{\frac{1}{2}} n^{\frac{3}{2}} A D_{i,\alpha}^{\frac{1}{2}} c_{i,\alpha}^* \nu^{\frac{1}{2}} \quad [\text{S1}]$$

where  $A$ ,  $F$ ,  $R$ ,  $T$ , and  $n$  are the interfacial surface area, Faraday's constant ( $96485.33 \text{ C mol}^{-1}$ ), Universal gas constant ( $8.314 \text{ J mol}^{-1} \text{ K}^{-1}$ ), absolute temperature ( $298.15 \text{ K}$ ), and the charge on the ion transferred (+1), respectively.  $D_{i,\alpha}$  and  $c_{i,\alpha}^*$  are the diffusion coefficient and initial/bulk concentration of species  $i$  in phase  $\alpha$ . The diffusion coefficient of  $\text{TEA}^+$  in water was taken to be  $9.8 \times 10^{-6} \text{ cm}^2 \text{ s}^{-1}$ .<sup>3</sup>  $i_p$  was plotted against  $v^{1/2}$  in Figure S2. Using the slope obtained from linear regression analysis in Figure S2 (dashed line), the radius of the microchannel was calculated to be  $\sim 11.9 \text{ }\mu\text{m}$  which is within experimental error of the commercially obtained  $12.5 \text{ }\mu\text{m}$  radius Pt wire used to form the microchannel.



**Figure S2:** Plot of  $i_p$  versus  $v^{1/2}$  from Figure S1. Dashed, red curve is the product of linear regression analysis with an  $R^2$  value of 0.998.

## 2. Asymmetric Diffusion Regime

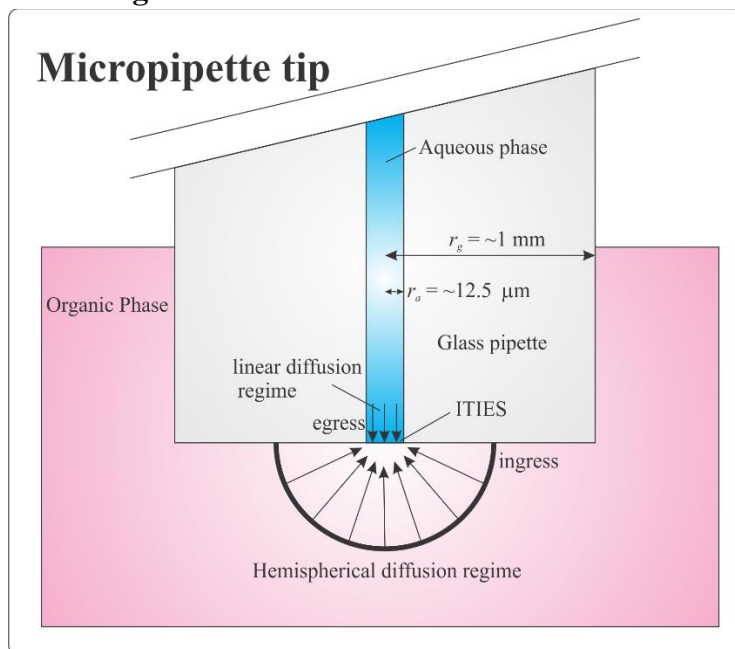


**Figure S3:** Schematic of the asymmetric diffusion regimes for egress and ingress of material across the ITIES held at the tip of a micropipette with external glass radius ( $r_g$ ) and an internal microchannel radius ( $r_a$ ) as indicated.

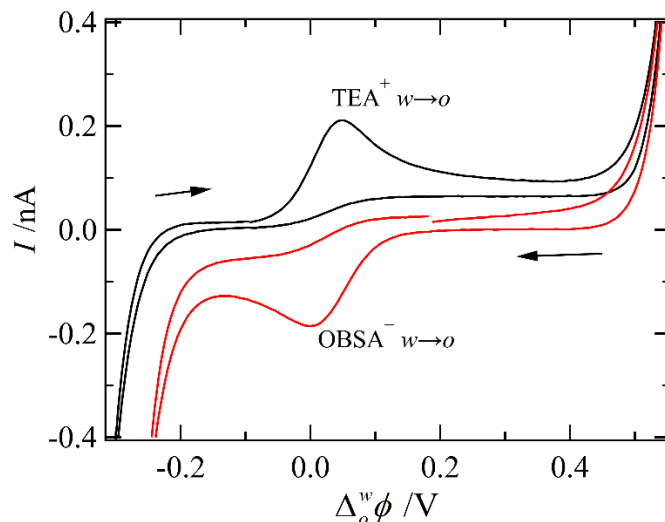


**Figure S4:** CVs recorded using Cell S1 and S2 with a scan rate of 25 and 50  $mV s^{-1}$  for the black and red trace demonstrating the  $TEA^+$  (tetraethylammonium) and  $OBSA^-$  (4-octylbenzenesulfonate) asymmetric ion transfer peak current responses, respectively, based on charge and the pipette geometry as shown in Figure S3.

### 3. Investigation of proton sources on ligand complexation

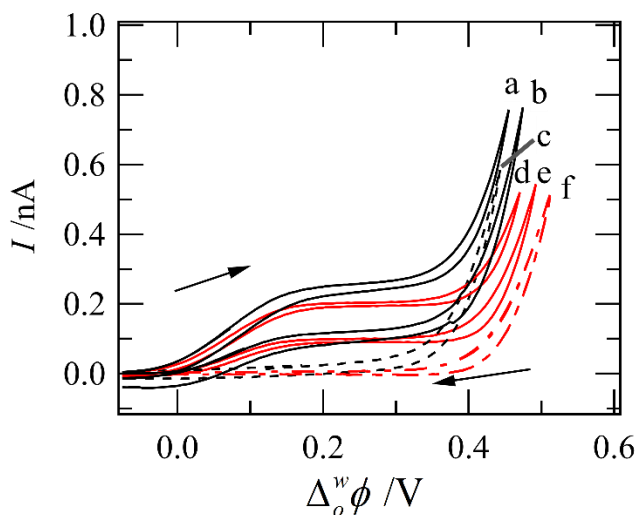


**Figure S5:** CVs using Cells 1 (curves d, e, f) and 2 (curves a, b, c) with the pH adjusted to 3.5 using HCl and citric acid, respectively, and  $L = HHQ$  at 25 (b and e) and 50  $\mu M$  (a and d). Curves c and f were recorded without HHQ in the DCE phase (blank curves). All other experimental parameters are the same as in Figure 1 of the main text.

#### 4. Cyclic voltammetric response moving from $[H^+] \gg [ligand]$ to the $[H^+] \approx [ligand]$ regime

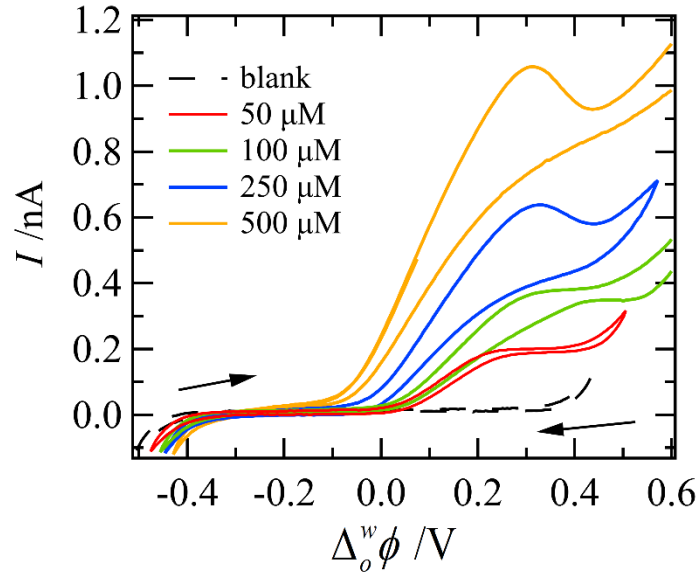


**Figure S6:** CVs recorded using Cell 1 with  $L = HHQ$  and  $[HHQ]$  varied from 0-500  $\mu M$  as indicated inset with a scan rate of  $25 \text{ mV s}^{-1}$ .

#### 5. Linear regression error analysis

The upper and lower associated error with the *line-of-best-fit* (LOBF) was determined using a method described in Skoog *et al.*<sup>4</sup> where the standard deviation ( $s_c$ ) about the LOBF is defined as,

$$s_c = s_r \sqrt{\frac{1}{N} + \frac{N(x - \bar{x})^2}{N \sum x^2 - (\sum x)^2}}$$

where  $s_r$  is the standard error from linear regression statistics and the upper and lower error bounds are,

$$\text{Upper LOBF+} = y = mx + b + ts_c$$

$$\text{Lower LOBF-} = y = mx + b - ts_c$$

In this case,  $t$  is students  $t$  value taken from standard tables using a 99.8% confidence interval and *degrees-of-freedom* as defined as  $N-2$ , where  $N$  is the population or number of data points used to construct the curve.

## References

1. Z. Samec, *Pure Appl. Chem.*, 2004, **76**, 2147-2180.
2. A. J. Bard and L. R. Faulkner, *Electrochemical Methods: Fundamentals and Applications*, John Wiley, New York, 2nd edn., 2001.
3. J. Strutwolf, M. D. Scanlon and D. W. M. Arrigan, *Analyst*, 2009, **134**, 148-158.
4. D. A. Skoog, *Principles of instrumental analysis*, Fourth edition. Fort Worth : Saunders College Pub., [1992] ©1992, 1992.